Magnetoacoustoelectronic instabilities in bismuth in constant and high-frequency electric fields

S. A. Vitkalov, V. F. Gantmakher, and G. I. Leviev

Institute of Solid State Physics, USSR Academy of Sciences
(Submitted 29 December 1985)
Zh. Eksp. Teor. Fiz. **90**, 2233–2240 (June 1986)

Experiments on bismuth were performed and a theory was developed for the magnetoacoustoelectronic instabilities due to the simultaneous action of a constant and a microwave electric field. The *I-V* characteristics of bismuth plates in a strong magnetic field have two kinks. One is due to phonon generation near the plate surface, and the other to phonon generation in the bulk. The second kink vanishes when the sample is irradiated with a microwave electromagnetic field of frequency $\omega \approx 10$ GHz. This means that the electromagnetic field suppresses phonon generation by the supersonic Hall flux of the carriers. It is shown that this suppression comes into play earliest at frequencies somewhat higher than that of the pump. The constant field E, in turn, suppresses the threshold second-harmonic generation produced by hypersound amplification at the frequency ω at high amplitude of the microwave field. This is attributed to the Doppler shift of the frequencies at which the sound damping due to the pumping is negative.

1. INTRODUCTION

When the drift velocity v_d of the carriers in a crystal reaches the sound velocity, an acoustoelectronic instability is produced and leads to phonon generation. This effect was first observed by Hutson *et al.*[1] for CdS in strong electric fields. In a field $E_1 = sm/e\tau$, when the drift velocity $v_d^{(E)} = Ee\tau/m$ reached s, a kink appeared on the *I-V* characteristic and decreased its slope (e and m are the charge and mass of the carriers, τ is the momentum relaxation time). Esaki[2] observed in bismuth a kink on the *I-V* characteristic in crossed electric (E) and magnetic (H) fields, in a field E_2 in which the sound velocity reached the Hall drift velocity $v_d^{(H)} = cE/H$. At $v_d^{(H)} > s$ the characteristic became steeper.

The theory of these instabilities is usually constructed in the magnetohydrodynamic approximation for an electron-hole plasma with allowance for the interaction between the carrier system and the lattice (see, e.g., the reviews[3,4]). At $v_d > s$ the damping γ of the sound excitations in the lattice becomes negative, so that their amplitude increases.

The presence of a constant drift $v_d^{(H)} > s$ increases strongly the nonlinear response of the bismuth at high frequencies ω (Ref. 5). Experiments at a frequency $\omega/2\pi \approx 10$ GHz have shown that this effect is due to amplification of the hypersound at the frequency $\omega_s \approx \omega$. On the other hand, without a constant drift but at sufficiently high electromagnetic-wave amplitude E_ω, the threshold phenomena in the nonlinear response of liquid are also weaker, particularly in second-harmonic generation.[6,7] As shown in Ref. 8, these threshold phenomena are also connected with an acoustoelectronic instability, albeit a somewhat different one than in the case of constant drift. In this case the phonons are generated as a result of parametric instability. The instability threshold is governed by the damping level in the phonon system. Therefore, even though s remains the characteristic scale of the oscillation amplitude of the drift velocity v_ω, the ratio $v_\omega^{th}/s = E_\omega^{th}/E_2$ can be smaller as well as larger than unity (v_ω^{th} and E_ω^{th} are there threshold values of the amplitudes v_ω and E_ω).

Our main purpose here was to investigate the joint action of two strong electric fields—constant (E) and alternating (E_ω). It turned out that such an action of parallel fields E and E_ω did not enhance the nonlinear phenomena, as might be expected, but weakened them. It can be seen from Fig. 1 that two manifestations of this weakening are observed. Increasing the amplitude E_ω to values comparable with but still weaker than E_2 causes the kink in field E_2 to vanish. On the other hand, application of a sufficiently strong constant field suppresses the second-harmonic generation, i.e., according to Ref. 8, the generation and amplification of the hypersound.

In addition, we report and discuss briefly two incidentally observed experimental facts. The *I-V* characteristics of bismuth plates cast in quartz molds exhibited in strong magnetic field an additional kink in a field $E_1 < E_2$. We shall

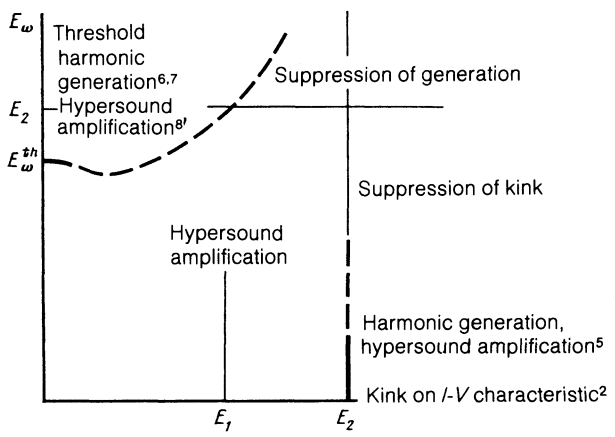

FIG.1

 0038-5646/86/061310-05$04.00

show that this kink is due to phonon generation in the subsurface layer of the bismuth plate. Near the field E_1 there is also observed a second-harmonic spike, just as near the field E_2. Its appearance, however, calls for a somewhat higher irradiation power P_ω.

After a brief discussion of some procedural problems, we report in the first two sections of the article the experimental results. In Sec. 3 we describe the I-V characteristic of bismuth, first in the absence and next in the presence of irradiation. We discuss here all the ideas concerning the nature of the kink in the field E_1, and return no more to this question. In Sec. 4 are reported the experimental data on the influence of the constant field E on the second-harmonic generation. This is followed in Sec. 5 by a theoretical model that describes the joint action of the constant and microwave electric fields. In the concluding part of the article we discuss from a point of view of this model all the experimental results connected with the presence of microwave irradiation.

2. EXPERIMENT

A bismuth sample measuring $18\times6\times0.4$ mm was irradiated through a diaphragm of 4 mm diameter by an electromagnetic field of frequency $\omega/2\pi = 9.1$ GHz. In addition, direct current J was made to flow through the sample, i.e., a constant field E was applied (see the inset of Fig. 2). To prevent overheating, both fields were applied in pulses. It was possible to vary the durations of both pulses and to shift one relative to the other. We measured the I-V characteristic and the second-harmonic power generated by the sample. The experimental setup is described in detail in Refs. 5 and 8.

In strong magnetic fields $H \gtrsim 40$ kOe the length of the magnetoplasma wave at 10 GHz is so large that it exceeds double the plate thickness $2d \approx 0.8$ mm. Under these conditions the electromagnetic-wave field in the sample can be regarded as uniform and can be estimated from the simple relation $E_\omega \approx \zeta H_\omega = (V_\alpha/c)H_\omega$ (V_α is the velocity of the magnetoplasma wave). The magnetic field H_ω is specified in the experiment (it does not depend on the sample impedance ζ) and is determined by the resonator figure of merit $Q \approx 10^3$, by its mode (TE_{101}), and by the incident power P_ω. Knowing these values, we can determine the electric field E_ω in the sample at an accuracy we estimate to be 50%.

The bismuth sample was cast in a demountable quartz mold. No additional surface treatment was used. This sample was used in Ref. 8 and assigned there the number 1.

All the experiments were performed at 4.2 K.

3. CURRENT-VOLTAGE CHARACTERISTIC OF BISMUTH

The solid line in Fig. 2 shows the I-V characteristic of the bismuth prior to exposure to the electromagnetic field. It has two kinks. The one on the right side was observed many times, starting with Refs. 2 and 9. When the field H is varied, this kink shifts in accordance with the formula $E_2 = (s/c)H$. The E_2 kink is preceded by a kink of opposite sign in a field $E_1 < E_2$, similar to that observed in CdS without a magnetic field.[1] The position of the E_1 kink depends little on H, but in weak fields it is less pronounced and is hard to distinguish against the background of E_2 kink that shifts with decreasing H towards weaker electric fields. Control experiments with a magnetic field $\mathbf{H}\|\mathbf{n}$ along the normal to the surface have shown that at this field configuration the E_1 kink vanishes but the E_2 kink remains.

Figure 3 shows the process of establishment of the stationary value of the current. It can be seen that the time connected with the E_1 kink is at least half the settling time at $E > E_2$. It is nevertheless still of the order of several microseconds, both in the Esaki effect[9] and in CdS.[1] The damping of the current after the drawing field is turned off also recalls the analogous process in CdS.[10]

All the characteristics of the kink of E_1 (the sign of the change of the resistance past the kink, the current settling

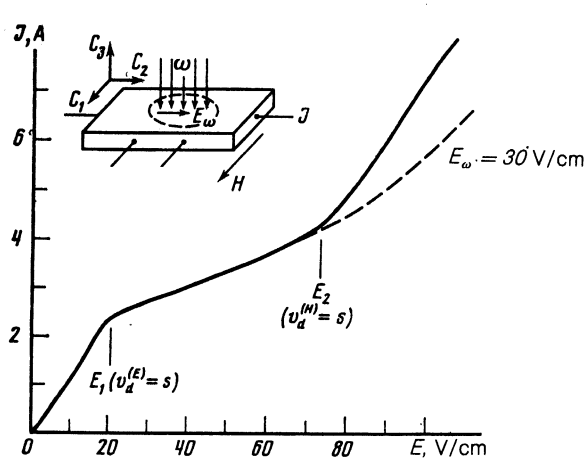

FIG. 2. Dependences of the current through the sample on the applied electric field E without irradiation (solid curve) and under conditions of microwave irradiation (dashed), $H = 60$ kOe. The dashed line in the inset shows the sample region irradiated by the microwave field.

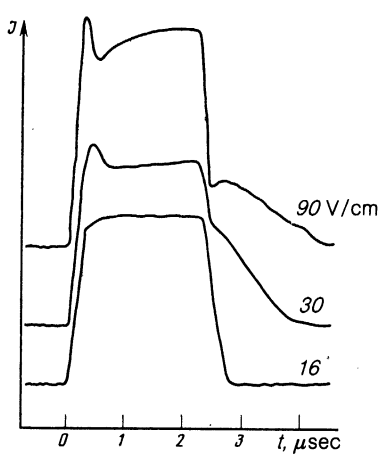

FIG. 3. Time dependence of current flowing through the sample at different values of E. The scales along the J axis are chosen such that the pulse sizes are approximately equal; $H = 60$ kOe, $E_\omega = 0$.

times, the sign of the residual current after turning off the drawing field) are reminiscent of the CdS kink.

According to Ref. 11, one of the variants of the static skin effect[12] is realized in bismuth in a magnetic field $\mathbf{H} \perp \mathbf{n}$. First, owing to the collisions with the surface, the displacements of the electrons along $\mathbf{E}$ directly at the surface are substantially stronger than in the bulk. Second, owing to the relatively low probability of the intervalley transitions (of the electron-hole recombination), $1/\tilde{\tau} \ll 1/\tau$, the drift of the electrons and of the holes $v_d^{(H)}$ leads to a carrier-density gradient at the surface.[13] As a result, the current is concentrated in a layer $h \approx R(\tilde{\tau}/\tau)^{1/2}$ at the bismuth surface (R is the Larmor radius). According to measurements,[11] $(\tilde{\tau}/\tau)^{1/2} \approx 10$, so that in fields $H \approx 50$ kOe we have $h \approx 10^{-4}$–10^{-5} cm. Using the value of the critical current from Fig. 2 ($J \approx 2.5$ A) and the known carrier density in bismuth, we find that the condition $v_d^{(E)} \approx s$ is indeed realized in a field $E \approx E_1$.

In Ref. 2, and also in later experiments (e.g., Refs. 9 and 14), the E_1 kink could not be observed for a number of reasons. First, the samples used in these experiments were cut by the electric-spark method, so that mechanical defects could make the intervalley scattering $\tilde{\tau} \approx \tau$ strong on the surface layer. Second, weaker magnetic fields were used in a number of cases. Third, the field E_1 might have been anisotropic and strongly dependent on the $\mathbf{n}$ direction. *Influence of the irradiation.* The dashed curve in Fig. 2 shows the influence of the irradiation on the I-V characteristic. The microwave field did not manifest itself in this characteristic in the region $E \sim E_1$, but did straighten out the kink at $E > E_2$. The same effect can be tracked also in Fig. 4. At $E_1 < E < E_2$ a field $E_\omega \approx 30$ V/cm does not affect the current J (lower pulse), but at larger E the same high-frequency field alters J (upper pulse).

Figure 4 excludes the possibility of attributing this influence to a change of the transverse conductivity σ_{xx} through heating of the crystal or of the carrier system by the field E_ω. Heating of the carrier system should increase rather than decrease $\sigma_{xx}(T)$ in a magnetic field, in view of the increase of the collision frequency $1/\tau$, and should have appeared on the lower curve, since both kinks are equally sensitive to temperature. Furthermore, processes that heat the entire crystal should lead to longer transient characteristics than observed in experiment (Fig. 4).

4. SECOND-HARMONIC GENERATION

It was shown in Refs. 5 and 8 that harmonic generation in the presence of a field $E > E_2$, or without a field E but in a strong electromagnetic field E_ω, proceeds in the same manner: the electromagnetic wave incident on the surface initiates a sound wave of frequency ω (Ref. 15); owing to the acoustoelectronic instability, the sound is amplified and is transformed into higher acoustic harmonics; hypersonic waves of multiple frequencies are again transformed into electromagnetic ones.

We report in this section the results of experiments on second-harmonic generation under simultaneous action of two fields, E and E_ω. The experimental curves are shown in Figs. 5 and 6. It can be seen from both figures that at small E_ω ($E_\omega \approx 0.3$ V/cm) generation takes place only at $E > E_2$ (the difference in the position of the generation peak on the E scale is due to the difference in the values of the constant field H). Increasing the amplitude E_ω leads to the appearance of an additional generation peak on the first kink $E \approx E_1$ (Fig. 5).

If $E_\omega > E_\omega^{th}$, harmonic generation sets in at $E = 0$. The electric field E changes the generation threshold. An example of such a change is shown in Fig. 7; the threshold is first lowered, and then begins to rise rapidly. The rise of the

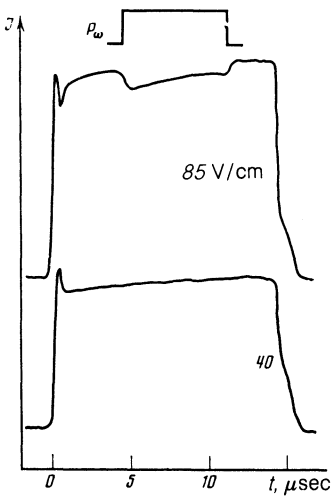

FIG. 4. Influence of microwave irradiation on the time dependence of the current flowing through the sample at different values of E; $E_\omega \approx 30$ V/cm, $H = 60$ kOe.

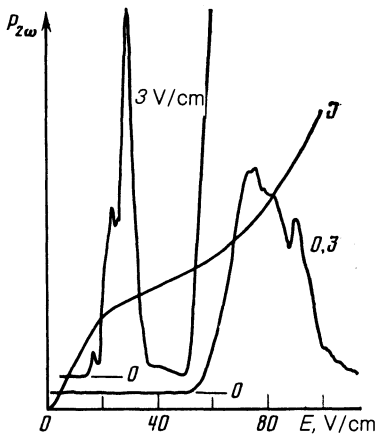

FIG. 5. Dependence of the second-harmonic power $P_{2\omega}$ on E at various amplitudes E_ω. Both curves were plotted for equal sensitivity of the receiving channel at the frequency 2ω. To compare the positions of the generation flashes the figure shows also the I-V characteristic; $H = 60$ kOe.

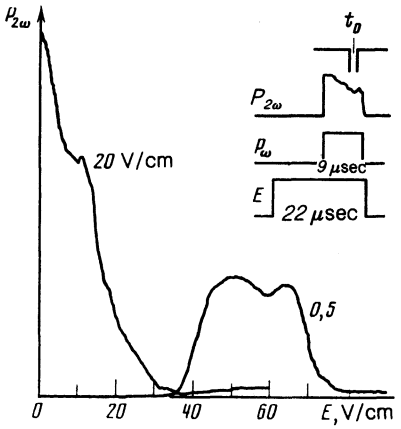

FIG. 6. Suppression of the parametric excitation of hypersound and of the harmonic generation by a constant electric field (curve at $E_\omega = 20$ V/cm); $H = 45$ kOe. For comparison, a plot of $P_{2\omega}(E)$ is shown for small E_ω. The inset shows the time t_0 elapsed from the start of the pulse and the instant when the power was measured.

threshold means that the second-harmonic power $P_{2\omega}$ decreases at a fixed pump level. This decrease of $P_{2\omega}$ on introduction of the field E is demonstrated in Fig. 6 at a pump level $E_\omega = 20$ V/cm.

Thus, at low pump amplitude the $P_{2\omega}$ generation takes place only at $E \simeq E_2$.[5] One more generation region appears next—near E_1. Finally, the maximum generation level for the largest pump amplitude E_ω takes place at $E = 0$, and E_ω decreases with increase of E.

5. THEORY

A coupled system of equations for a magnetized electron-hole plasma in a neutral lattice was derived in Ref. 8. It is applicable in a sufficiently strong magnetic field: $qR \ll 1$ and $\Omega \gg \omega \gg 1/\tau$, where Ω and R are the cyclotron frequency and the radius, while q is the wave vector of the transverse magnetic field. This system was solved in Ref. 8 to investigate acoustic instabilities in the presence of strong homogeneous ($k = 0$) electromagnetic pumping. It turned out that pumping near frequencies $n\omega$ that are multiples of the pump frequency gives rise to narrow frequency regions

$$n\omega - \nu_n \leqslant \omega_s < n\omega, \quad \nu_n = \frac{(qR)^2}{3\tau} = \frac{1}{3\tau}\left(\frac{n\omega}{\Omega}\right)^2\left(\frac{v_F}{s}\right)^2, \quad n = 1, 2, \ldots, \tag{1}$$

in which the sound damping rate is negative, $\gamma < 0$.

Let us generalize the solution given in Ref. 8, by introducing besides the alternating carrier drift with velocity $v_\omega \cos \omega t = c(E_\omega/H)\cos \omega t$ also a constant drift in the same direction, with velocity

$$v_d = cE/H. \tag{2}$$

The electromagnetic pumping is assumed homogeneous as before. We define the moving coordinate frame introduced in the course of the solution as

$$\xi = y - v_d t - (v_\omega/\omega)\sin \omega t, \tag{3}$$

where y is the coordinate in the immobile system along the axis $y \| \mathbf{v}_d \| \mathbf{v}_\omega \perp \mathbf{H}$. The sound wave

$$u = (u_{q0}/2)\exp i(qy - \omega_s t) \tag{4}$$

is transformed in the new coordinate system into

$$u^* = (u_{q0}/2)\exp(i\xi q)\exp i[(qv_d - \omega_s)t + (qv_\omega/\omega)\sin \omega t]. \tag{5}$$

Following next the procedure of Ref. 8 and using Ref. 16, we obtain the sound-wave damping (4) in the form

$$\gamma = \gamma_0 \omega_s \sum_{n=-\infty}^{\infty} \frac{\omega_s(1 - v_d/s) - n\omega}{[\omega_s(1 - v_d/s) - n\omega]^2 + \nu^2} J^2\left(\frac{\omega_s}{\omega}\frac{v_\omega}{s}\right), \tag{6}$$

$$\gamma_0 = \frac{2Q^2N}{m\rho s^4\tau}\left(\frac{\omega_s}{\Omega}\right)^2, \quad \nu = \frac{(qR)^2}{3\tau} = \frac{1}{3\tau}\left(\frac{\omega_s}{\Omega}\right)^2\left(\frac{v_F}{s}\right)^2,$$

where N is the equilibrium carrier density, Q the arithmetic mean of the electron and hold deformation potentials, m and v_F the electron mass and Fermi velocity, and ρ the bismuth density.

It follows from (6) that the set of frequencies near which the sound damping by the pump becomes negative, undergoes a Doppler shift

$$\omega_{sn} = n\omega/(1 - v_d/s), \quad n = 1, 2, \ldots. \tag{7}$$

6. DISCUSSION

Linearization of the current-voltage characteristic. For sound frequencies

$$\omega_s \ll \omega/|\mu|, \quad \mu = 1 - v_d/s$$

Eq. (6) can be written in the form

$$\gamma = \gamma_0 \mu\left[\frac{\omega_s^2}{(\mu\omega_s)^2 + \nu^2} J_0^2(z) - \left(\frac{\omega_s}{\omega}\right)^2 S(z)\right], \quad z = \frac{\omega_s}{\omega}\frac{v_\omega}{s}, \tag{8}$$

where

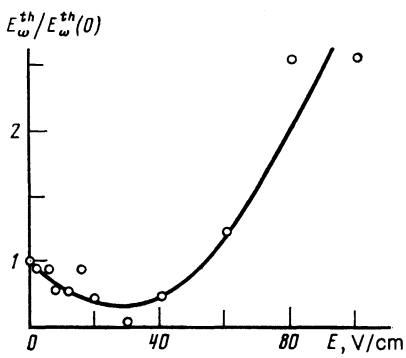

FIG. 7. Dependence of the threshold E_ω^{th} on the constant field E; $H = 46$ kOe.

$$S(z)=2\sum_{n=1}^{\infty}\frac{1}{n^2}J_n^2(z)<1, \quad S(0)=0. \tag{9}$$

We are interested in the region above the kink of the *I-V* characteristic, where $\mu<0$ and $|\mu|\approx 0.1$–0.5. If there is no pump, (8) goes over into the known equation that describes the acoustoelectronic instability in crossed fields.[3,4] The coefficient γ is negative in the entire frequency band ($qR<1$, i.e., $\omega_s<\omega_{s\max}=(s/v_F)\Omega$), where the effective electron-phonon interaction is produced. The kink is due to phonon emission in the entire frequency interval from zero to $\omega_{s\max}$ and the largest contribution is made by high-frequency phonons that acquire a maximum momentum from the electron system.

In our case

$$\omega_{s\,max}\approx\omega/|\mu|\approx(2-10)\,\omega,$$

so that Eq. (8) can be used for the entire frequency interval from 0 to $\omega_{s\max}$. It can be seen from (8) that turning-on the pump suppresses the instability in fact at the high frequencies. For example, for the experimental curve on Fig. 2 we have $v_\omega/s\approx 0.5$, and $\mu=-0.3$ corresponds to the point with the abscissa 100 V/cm. According to (8), the high-frequency pump decreases $|\gamma|$ under these conditions by approximately 15% at the frequency $\omega_s=\omega$, by more than a factor of two at $\omega_s=2\omega$, and the coefficient γ becomes positive at $\omega_s>2.5\,\omega$.

Figure 2 contains one more important experimental fact: low frequency pumping had no effect whatever on the kink in the field E_1. We assume that this difference in the action of the pump on different sections of the *I-V* characteristic is due to differences in the modulation depth β of the drift velocity. The buildup time of the velocity $v_d^{(H)}$ is very short, of the order of $\Omega^{-1}\ll\omega^{-1}$. Therefore the relative modulation depth is $\beta=v_\omega/v_d^{(H)}=E_\omega/E$. The buildup time of the subsurface current, determined by diffusion and interband recombination, is equal to $\tau_s\approx(\tilde{\tau}\tau)^{1/2}\gg\omega^{-1}$. This decrease β by a factor $\omega\tau_s$, i.e., at least by two orders.

Suppression of harmonic generation. The negative sound damping near the pump frequency is determined by the term having $n=1$ in the sum of (6). The maximum instability growth rate $-\gamma_m$ is realized at the frequency

$$\omega_{s1}=\frac{\omega-\nu_1}{1-v_d/s}, \quad \nu_1=\nu|_{\omega_s=\omega}=\frac{1}{3\tau}\left(\frac{\omega}{\Omega}\right)^2\left(\frac{v_F}{s}\right)^2, \tag{10}$$

which is less than ω at $v_d=0$, and then increases rapidly with increasing v_d. The initiating sound wave that is amplified in our experiments has a frequency ω. This means that the Doppler shift of the frequency ω_{s1} first improves the agreement between the initiating sound and the natural frequency of the hypersound amplifier, and then causes a complete mismatch between them at $v_d/s>\nu_1/\omega$. At a small value of ν_1/ω, i.e., in stronger fields H, the initial growth of the gain may even not set in. All these conclusions are in fact confirmed by the experimental curves in Fig. 6 and 7.

The foregoing explanations confirm once more the correctness of the initial assumption formulated in [8]: second-harmonic generation is due precisely to amplification of weak sound at a frequency ω, generated on the surface, and not to generation of sound in the bulk in the immediate vicinity of the frequency 2ω on account of the negative γ in the second frequency interval (7).

Second harmonic generation on the kink E_1. It appears that the mechanism whereby a harmonic is generated on the kink E_1 is similar to the mechanism considered in Ref. 5 for the kink E_2. There is an obvious difference in the volume occupied by the active medium: in the field $E\approx E_1$ this is only a layer of thickness h. Observation of this generation requires therefore a higher incident power P_ω. At the same time, there should be also other differences, connected in particular with the fact that the wave vector of the amplified sound should be directed along the surface. This question calls for further study.

The authors are grateful to S. S. Murzin for a discussion of the results and for supplying the sample.

[1]A. R. Hutson, J. H. McFee, and D. L. White, Phys. Rev. Lett. **7**, 237 (1961).
[2]L. Esaki, *ibid.* **8**, 4 (1962).
[3]H. Spector, Solid State Physics (F. Seitz and D. Turbull, eds. Vol. 19, p. 291 (1966).
[4]V. I. Pustovoit, Usp. Fiz. Nauk **97**, 257 (1969) [Sov. Phys. Usp. **12**, 105 (1969)].
[5]S. A. Vitkalov, V. F. Gantmakher, and G. I. Leviev, Sol. St. Commun. **54**, 1091 (1985).
[6]E. G. Yashchin, Fiz. Tverd. Tela (Leningrad) **22**, 1740 (1980) [Sov. Phys. Solid State **22**, 1014 (1980)].
[7]S. A. Vitkalov, V. F. Gantmakher, and G. I. Leviev, Pis'ma Zh. Eksp. Teor. Fiz. **39**, 540 (1984) [JETP Lett. **39**, 660 (1984)].
[8]S. A. Vitkalov, V. F. Gantmakher, and G. I. Leviev, Zh. Eksp. Teor. Fiz. **90**, 1493 (1986) [Sov. Phys. JETP **63**, No. 4 (1986)].
[9]T. Yamada, J. Phys. Soc. Japan **20**, 1647 (1965).
[10]J. H. McFee, J. Appl. Phys. **34**, 1548 (1963).
[11]S. S. Murzin, Zh. Eksp. Teor Fiz. **82**, 515 (1982) [Sov. Phys. JETP **55**, 298 (1982)].
[12]M. Ya. Azbel', *ibid*, **44**, 983 (1963) [**17**, 667 (1963)].
[13]E. I. Rashba, Z. S. Gribnikov, and V. Ya. Kravchenko, Usp. Fiz. Nauk **119**, 3 (1976) [Sov. Phys. Usp. **19**, 361 (1976)].
[14]Yu. A. Bogod and R. G. Vasil'ev, Fiz. Nizk. Temp. **7**, 897 (1976) [*sic*].
[15]A. I. Vasil'ev and Yu. P. Gaidukov, Usp. Fiz. Nauk **141**, 431 (1983) [Sov. Phys. Usp. **26**, 952 (1983)].
[16]M. Cohen, M. J. Harrison, and W. A. Harrison, Phys. Rev. **117**, 937 (1960).

Translated by J. G. Adashko